

CIRP Conference on Manufacturing Systems (CIRP CMS)

# Profile Characterization of Low-Temperature Niobium Depositions in Vented-Nozzle Cold Spray

Arun Ruhfus<sup>a</sup>, Liam McAuliffe<sup>a</sup>, Ronnie F. P. Stone<sup>a</sup>, Desiderio Kovar<sup>a</sup>, Zhenghui Sha<sup>a,\*</sup><sup>a</sup>Center for Additive Manufacturing and Design Innovation, Walker Department of Mechanical Engineering, The University of Texas at Austin, TX 78712\* Corresponding author. Tel.: +1-512-471-1818. E-mail address: [zsha@austin.utexas.edu](mailto:zsha@austin.utexas.edu)

## Abstract

Cold spray is an emerging additive manufacturing technology with great potential in the solid freeform fabrication of parts with complex geometries. While cold spray manufacturing with conventional converging-diverging nozzles has had success with softer metals, it has struggled to produce quality films and coatings from hard metals or ceramics. Vented nozzle designs, recently developed for micro-cold spray applications, offer a potential solution to this issue, as they allow for significantly less abrasive, finer powders (e.g., 1–5  $\mu\text{m}$ ) to be used. Vented nozzles incorporate pressure relief channels that enhance particle deposition velocity and enable deposition at comparatively lower temperatures than converging-diverging nozzles (i.e., from 450°C to 200°C). However, a comprehensive profile characterization of vented nozzle depositions in cold spray is lacking in the literature. As such, this work fills this gap by presenting the first comprehensive investigation of the profile characteristics of vented nozzles using high-purity niobium powder. To study the profile of vented nozzle depositions, a full factorial design of experiments was employed to evaluate the effects of the number of passes and standoff distance, two critical features in cold spray shape control analysis. After depositing track lines for each set of process parameters, the cross-sectional profiles were characterized using optical profilometry and fit using exponential-family distributions. Results demonstrate that vented nozzle depositions exhibit characteristic Gaussian profile distributions consistent with conventional cold spray, suggesting that established modeling frameworks remain applicable despite fundamentally altered gas flow dynamics. These preliminary findings are promising as they suggest that vented nozzles can be more readily integrated into cold spray additive manufacturing applications, leveraging lower-temperature deposition while providing a pathway into broader material compatibility with hard metals and ceramics.

© 2025 The Authors. Published by Elsevier B.V.

This is an open access article under the CC BY-NC-ND license (<http://creativecommons.org/licenses/by-nc-nd/4.0/>)

Peer-review under responsibility of the scientific committee of the 2025 CIRP CMS.

**Keywords:** Additive Manufacturing; Cold Spray; Surface Morphology; Vented Nozzles; Low-Temperature Processing

## 1. Introduction

Cold spray (CS) is a solid-state spraying method where particles, typically close to 50  $\mu\text{m}$ , are accelerated to supersonic velocities (i.e., between 300 and 1200  $\text{m/s}$ ) through a converging-diverging nozzle, leading them to impact and adhere to a substrate of choice through the conversion of kinetic energy to plastic deformation during the bonding process [21]. Developed in the 1980s in Russia, this technology has undergone extensive development and now serves critical applications across the aerospace, automotive, defense, and biomedical sectors [11]. The solid-state nature of the CS process produces oxide-free deposits, preserves feedstock material characteristics, and prevents substrate thermal degradation, attributes that are difficult to achieve through traditional thermal spray methods [2, 26].

CS typically requires a combination of high gas temperatures (up to 900°C) and high particle velocities to achieve sufficient bonding due to the *critical impact velocity* phenomenon [19]. The feasible operating window can be further restricted because of gas stagnation that occurs upstream of the substrate surface that significantly reduces particle velocity, particularly for fine particles (i.e., < 10  $\mu\text{m}$ ) [3]. Recent studies in micro-cold spray (MCS), a lower-pressure variant of CS that operates with comparatively finer particles (i.e., 30 nm – 2  $\mu\text{m}$ ) deposited in a rough technical vacuum environment [1, 12], have demonstrated that introducing pressure relief channels (see Figure 1) to the nozzle design can significantly reduce particle slowing allowing for higher particle impact velocities and an expanded operational parameter window [8, 4, 3]. Thus, this *vented nozzle* architecture represents a promising approach to deposit harder

2212-8271 © 2025 The Authors. Published by Elsevier B.V.

This is an open access article under the CC BY-NC-ND license (<http://creativecommons.org/licenses/by-nc-nd/4.0/>)

Peer-review under responsibility of the scientific committee of the 2025 CIRP CMS.

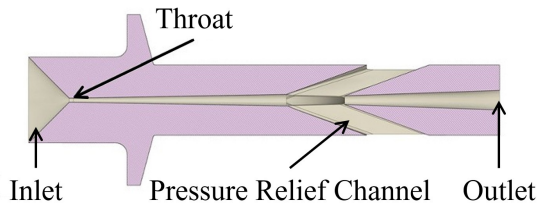


Fig. 1: Cross-sectional View of Vented Nozzle Design

metals and ceramics in CS, enabling deposition at lower temperatures and accommodating a wider range of materials.

To enable widespread adoption of vented nozzles in the CS community, comprehensive characterization of their deposition profiles is essential, particularly for hard metals and ceramics relevant to additive manufacturing applications. In recent years, CS has been increasingly leveraged as an additive manufacturing technology (CSAM) [29], yet surface morphology control of deposited features, which significantly affects deposition efficiency and final part quality [27], remains a fundamental challenge limiting feature resolution and robust control of complex geometries compared to alternative metal AM processes [10]. While various research groups have addressed this problem using standard De Laval nozzles, no work has examined vented nozzle architectures. This study aims to bridge this knowledge gap by presenting the first comprehensive characterization of vented nozzle deposition surface morphology, providing a foundation for CSAM with vented nozzles and enabling manufacturing of metallic and ceramic free-standing components.

The remainder of this paper is organized as follows: a brief literature review of deposition profile studies is presented in Section 2. The methodology and design of experiments are outlined in Section 3. A summary of the results is presented in Section 4, and, finally, current limitations and future research directions are discussed in Section 5.

## 2. Related Work

While our work is uniquely focused on the surface morphology investigation produced using vented nozzle designs, there is a wealth of literature on CS shape and geometry control [10]. The work can be broadly categorized as Gaussian fit models, physics-based predictors, and data-driven models.

Gaussian fit models leverage the Gaussian nature of the profile in CS depositions, which form due to the axisymmetric geometry of the nozzles radially influencing particle velocities [6]. As such, using experimental data, it is possible to relate the parameters of the Gaussian profile (e.g., standard deviation) to a CS process parameter of interest (e.g., standoff distance) and infer its impacts on relevant performance metrics, such as deposition efficiency and coating thickness [5]. Notably, a Gaussian model can also accurately predict profiles in off-normal spray angle depositions by transforming the profile into a polar coordinate system, naturally capturing the experimentally observed deposition efficiency loss at shallower deposition angles [7]. Finally, Gaussian fits are not exclusive to CS and have been ex-

plored in other thermal spray studies [18, 24]. Despite the success of Gaussian fits in modeling CS depositions, it has been observed that their prediction accuracy diminishes as more layers are deposited. This is due to a number of factors, including the well-established *shadow effect* and the local curvatures of the deposition area, which can be addressed numerically, albeit at a higher computational cost [28].

Physics-based models attempt to address the predictive limitations of the Gaussian fits by incorporating knowledge of the deposition physics. This can be achieved by relating the growth of the profile over time using differential equations, which can then be solved numerically to predict the material buildup over multiple layers of varying local curvatures [16, 17]. Advanced models which incorporate standoff distance (SOD) and shadow effects have also been proposed and experimentally validated, although the main concerns remain the high computational cost, the need to estimate certain coefficients in the differential equation based on experimental data, and the uncertainties derived from nozzle alignment [25, 20]. The computational costs for real-time generation of toolpaths can be reduced using data-driven approaches. For example, simple Gaussian process regression and multi-layer perceptron models have been successfully trained and validated in different CS applications [13, 15]. However, the primary concern is the dependence of the models on the dataset, which requires large sets of experimental data or data-efficient approaches with limited applicability [14].

## 3. Methodology

### 3.1. Design of Experiments

Two process parameters can significantly influence the profile characteristics of CS depositions: how many times the nozzle deposits over the same area (i.e., number of passes), and the distance between the nozzle exit and the surface of the substrate (i.e., SOD). Generally, multiple passes increase profile thickness and promote densification and grain refinement, though deposition efficiency (DE) typically decreases in subsequent passes as particles impact harder previously-deposited material rather than the softer substrate. Thus, the number of passes is critical in CSAM where solid, thick layers are required to manufacture freestanding parts. Similarly, there is a characteristic optimum SOD which maximizes DE. This is due to shorter SODs creating bow shock effects and flow disruptions, while large SODs result in particle deceleration and cooling due to gas jet dissipation and atmospheric drag. In both cases, the conditions can reduce the impact velocity below the critical threshold required for effective bonding. The optimal SOD range varies with particle size and material; shorter distances generally produce denser coatings with lower porosity due to higher impact velocities, whereas greater standoff distances result in broader spray footprints but lower coating density and potentially higher surface roughness. These well-documented relationships for conventional nozzles provide the essential baseline for the proposed design of experiments (DOE) for the vented nozzle.

A full factorial DOE was implemented, characterizing deposit profile evolution as a function of spray passes (2, 6, and 10) and SOD (3×, 5×, and 10× nozzle diameter) for niobium powder deposited at 200°C, significantly below conventional temperature requirements. The spray pass range was established through initial testing, which revealed Gaussian profile characteristics after just 2 passes. Ten passes was chosen to provide an upper limit that minimizes material waste, while 6 passes was selected for even spacing. The SOD levels were chosen based on operational constraints and characteristic optimization: 3× nozzle diameter represents the minimum distance without perceived bow shock effects that would disrupt gas flow and reduce particle impact velocity below critical bonding thresholds, 5× represents a reasonable standard operational distance balancing deposition efficiency with footprint characteristics, and 10× provides an extreme value where gas jet dissipation and atmospheric drag may reduce particle velocity and temperature. For each SOD, three samples were processed as a batch with different pass counts while maintaining fixed SOD, enabling efficient processing.

### 3.2. Cold Spray System and Process Parameters

All depositions were performed using a VRC GEN3.1 cold spray system equipped with a custom vented nozzle. High-purity niobium powder (99.8% purity) with an average particle size (APS) distribution of 1–5  $\mu\text{m}$  was deposited with a process gas temperature of 200°C and a system pressure of 435 psi (30 Bar), using nitrogen as the propellant gas. This highlights the key advantages of the custom developed nozzle as niobium is typically deposited with a temperature over 450°C, a comparison of the two processing windows can be seen in Table 2. [22, 23] Several process parameters were held constant throughout the experimental campaign to isolate the effects of the primary variables: traverse speed was maintained at 10 mm/s, spray angle was fixed at 90° relative to the substrate surface and the nozzle throat diameter was 1.75 mm. A full list of processing parameters can be seen in Table 1.

Table 1: Cold Spray Process Parameters

Parameter	Value	Unit
Carrier Gas	Nitrogen	
Carrier Gas Temperature	200	Celsius
Carrier Gas Pressure	435	Psi
Gantry Speed	10	mm/s
Standoff Distance	5.25, 8.75, 17.5	mm
Passes	2, 6, 10	
Material	Niobium	
Purity	99.8	%
Powder Size	1-5	Micron
Feeder Setting	5	rpm
Nozzle Throat Diameter	1.75	mm

Substrates consisted of 1/16-inch (1.59 mm) thick aluminum plates cut to 3 × 1.5 inches (76.2 mm × 38.1 mm). Individual samples were prepared by chopping longer strips to the

Table 2: Process Parameter Comparison

Parameter	Vented Nozzle	Conventional Nozzle
Pressure (PSI)	435	290
Temperature (°C)	200	≥450

specified length and then bolted to a custom sample holder designed to accommodate three substrates simultaneously. Prior to deposition, each substrate was carefully wiped with acetone to remove any contaminants that could affect coating adhesion.

Depositions were executed using a custom-built XY gantry stage system with the nozzle mounted in a fixed position while the substrate was translated beneath it. The system was first brought to steady-state operating conditions by running off the samples, then repositioned onto the sample to begin the deposition. Following deposition, samples were removed from the holder and cleaned in an ultrasonic bath. Each sample was placed in acetone and sonicated for two minutes to remove any loosely adhered material, ensuring that only sufficiently bonded niobium remained on the substrate for subsequent analysis.

### 3.3. Characterization and Data Acquisition

Deposit morphology and thickness measurements were obtained using a Keyence VHX-7000 digital microscope. To ensure statistical reliability and account for variation in the deposition characteristics, each sample was split into three similarly sized areas and one measurement was taken from each of these areas. Each measurement took the profile of the deposition perpendicular to the nozzle path, and used 5 individual profiles at 25  $\mu\text{m}$  spacing, averaged together to minimize the affects of larger aggregates on the final profile. This measurement process provided representative data across the entire deposit length while minimizing systematic bias from edge effects or localized anomalies.

All measurements were conducted at 100× magnification to achieve adequate resolution to accurately determine the thickness of the depositions. Initial imaging trials evaluated multiple illumination configurations, including coaxial and partial ring lighting, to optimize contrast and edge definition of the deposit profiles. Full-ring lighting was ultimately selected because it provided the most consistent and reliable detection across all samples, particularly for the irregular surface morphologies characteristic of cold-sprayed niobium deposits. The uniform illumination from the full-ring configuration minimized shadowing and enabled more accurate automated profile measurements than directional lighting schemes. An example of a deposition can be seen in Figure 3b.

### 3.4. Profile Correction Methodology

Tilt correction was employed using a custom Python script that was developed to process raw profile data by identifying the two flat substrate regions flanking each deposit, marked by the green and purple regions in Figure 2 and applying a transfor-

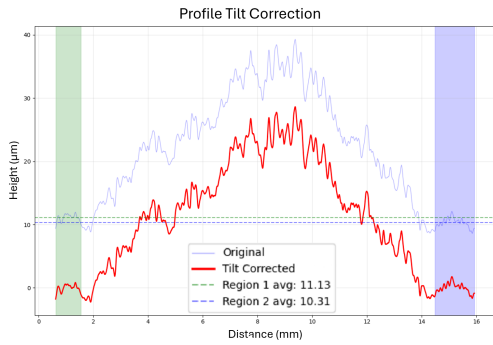


Fig. 2: Profile Correction and Zeroing Process

mation to render these areas horizontal and level, shown via the region 1 and 2 average heights. The baseline was subsequently zeroed to ensure that all height measurements represented true deposit thickness relative to the substrate surface.

## 4. Results and Discussions

### 4.1. Profile Distribution Characterization and Model Selection

To mathematically characterize the cross-sectional geometry of vented nozzle deposits, each corrected profile was fit to Gaussian, Beta, and Gamma candidate functions, truncated over the width of the dataset. The three functions were chosen for their ability to compactly represent complex curves and for the fact that distributions are commonly used to represent CS depositions, as discussed in Section 2. Fitting quality was assessed using the coefficient of determination ( $R^2$ ) averaged across the entire dataset, encompassing all combinations of SOD and pass count evaluated in the DOE. The comparative performance of all candidate functions is presented in Table 3.

The results are: Beta distribution ( $R^2 = 0.9766$ ), Gaussian distribution ( $R^2 = 0.9753$ ) and Gamma distribution ( $R^2 = 0.9126$ ). Despite the marginally superior performance of the Beta function, the Gaussian distribution was selected as the primary analytical framework for several reasons. First, the performance difference between it and the Beta function is minimal indicating negligible practical distinction in fitting quality. Second, Gaussian distributions represent the established standard for characterizing CS deposition profiles in the literature, enabling direct comparison with conventional nozzle systems and facilitating integration of these findings into the existing body of knowledge [10, 13, 14, 15, 16, 18]. Third, while the Beta distribution exhibited slightly higher average  $R^2$ , it demonstrated greater standard deviation across the dataset, suggest-

Table 3: Curve Fitting Results

Fitting Curve	Avg. $R^2$	Std. Dev.
Gaussian Distribution	0.9753	0.0173
Gamma Distribution	0.9126	0.0300
Beta Distribution	0.9766	0.0180

ing less consistent performance. Furthermore, Beta distributions are specifically designed to capture profile asymmetry and skewness, characteristics absent in the symmetric single-track deposits examined in this study, especially since the functions are truncated and centered on the dataset. Finally, the Gaussian formulation provides compact parameterization through only two physically interpretable parameters: amplitude ( $A$ ), representing maximum deposit height, and standard deviation ( $\sigma$ ), characterizing profile width.

### 4.2. Systematic Characterization of Deposition Behavior and Process Parameter Effects

Gaussian fitting quality across the complete design space (Table 4) demonstrated excellent consistency, with  $R^2$  values ranging from 0.9340 to 0.9905, with a dataset-wide mean of 0.9753. This demonstrates a key finding: vented nozzle deposits exhibit highly consistent Gaussian profile morphology regardless of SOD or pass count combinations. A representative deposition and profiles for 3x nozzle diameter SOD with 6 passes are shown in Figure 3, with Figure 3a illustrating the three extracted profiles and their Gaussian fits, exemplifying the methodology applied to generate all data in Table 4. Analysis of fitting variability revealed the lowest  $R^2$  ( $0.9340 \pm 0.0120$ ) at 17.5 mm SOD with 6 passes, exhibiting the highest standard deviation, while the highest  $R^2$  ( $0.9905 \pm 0.0024$ ) occurred at 17.5 mm with 10 passes, suggesting intermediate pass counts at high standoff distances introduce increased measurement scatter, potentially reflecting transitional deposition behavior or heightened process sensitivity.

Process parameters exhibited complex effects on deposit geometry. Pass count demonstrated non-monotonic behavior, with 6-pass depositions consistently yielding lower amplitudes than either 2-pass or 10-pass conditions across all standoff distances, suggesting competing mechanisms between peening/densification effects and continued material buildup. Deposit amplitude ranged from  $28.01 \pm 2.81 \mu\text{m}$  (17.5 mm, 6 passes) to  $88.89 \pm 5.22 \mu\text{m}$  (17.5 mm, 10 passes), representing multi-variate variation, but generally increasing with SOD. Profile width ( $\sigma$ ) exhibited similar non-monotonic pass count

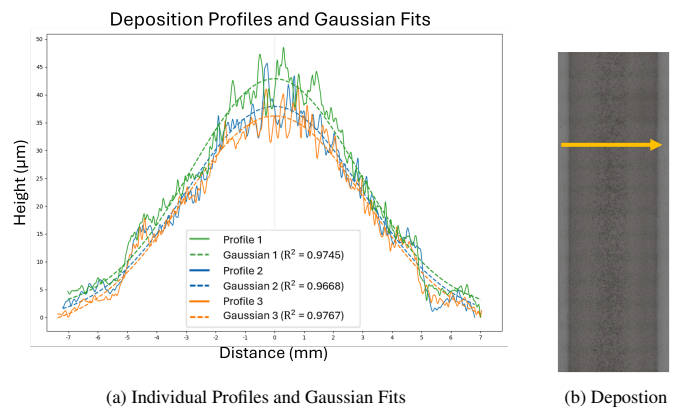


Fig. 3: Characterization of 3x Nozzle Diameter and 6 Passes Run, Yellow Arrow indicates direction of Profile Scan

dependence but demonstrated consistent, physically intuitive SOD effects:  $\sigma$  increased systematically from  $2.966 \pm 0.107$  mm at 5.25 mm to  $4.958 \pm 0.254$  mm at 17.5 mm, a 67% increase, attributable to gas jet expansion and divergence producing broader spray footprints at larger distances. The repeatability metrics represent inter-run variation within the current experimental round and require additional rounds of design of experiments to establish true process repeatability (see Table 4).

#### 4.3. Morphological and Microstructural Observations

Examination of deposit profiles revealed evidence of substrate erosion at the periphery of the spray track, manifesting as slight substrate depression prior to the onset of material buildup. This sandblasting-type phenomenon results from particle impacts with insufficient kinetic energy for bonding but adequate energy for surface erosion and material removal. The extent and consistency of this erosion zone varied both within individual samples and across different process conditions, suggesting sensitivity to local variations in particle velocity distribution and impact angle. The soft aluminum substrate employed is likely easier to erode than harder substrate materials, which represents an important consideration for future work examining substrate material effects on deposition behavior.

Optical microscopy analysis of the as-deposited coatings revealed a dense, cohesive film with visual evidence of effective interparticle bonding throughout the coating thickness. These observations suggest that adequate plastic deformation and mechanical interlocking occurred during the deposition process despite the significantly reduced gas temperatures employed relative to conventional CS systems.

#### 4.4. Implications for Vented Nozzle Technology

A key finding of this investigation is the preservation of characteristic Gaussian profile morphology in vented nozzle deposits despite the fundamentally altered gas flow dynamics introduced by the pressure relief channel architecture. This consistency suggests that the underlying mechanisms governing material deposition; plastic deformation, mechanical interlocking, and adiabatic shear instabilities, remain dominant even when the gas flow field is substantially modified relative to conventional De Laval nozzle designs. The significance of this finding extends beyond morphological similarity: it suggests that established modeling frameworks, empirical correlations, and process optimization strategies developed for conventional CS systems may be transferable to vented nozzle architectures with appropriate calibration. While systematic validation of this transferability remains an important area for future investigation, the preservation of fundamental deposition behavior provides an encouraging baseline for predictive modeling efforts and process development initiatives.

The vented nozzle architecture demonstrated a critical advantage in enabling low-temperature deposition of refractory metals. Successful deposition of niobium at  $200^\circ\text{C}$  represents a reduction of more than  $250^\circ\text{C}$  compared to conventional CS requirements, which typically necessitate gas temperatures ex-

ceeding  $450^\circ\text{C}$  for adequate niobium bonding. Despite this substantial reduction in thermal input, the deposits maintained adequate bonding characteristics and exhibited the profile quality documented throughout this study. The reduced temperature requirements present several other advantages for industrial implementation. In particular, it enables the potential use of compressed air as a propellant gas instead of bottled nitrogen. At traditional cold spray temperatures, Niobium operates within the linear oxidation regime, whereas with the reduced temperatures, it is firmly within the early parabolic oxidation regime, significantly reducing oxidation during particle flight and deposition [9]. For reactive materials such as titanium, aluminum, and niobium, where oxide formation can compromise coating properties, reduce bonding efficiency, and limit functional performance, the mitigation of in-flight oxidation through reduced thermal exposure offers a pathway to improved coating purity and enhanced functional properties.

Furthermore, these preliminary experiments conducted using the vented nozzle have demonstrated ceramic deposition capability under processing conditions similar to those employed in micro-cold spray applications. The ability to deposit ceramics through this approach could significantly expand the range of materials available for CPAM, particularly enabling the fabrication of components requiring hard, wear-resistant, or thermally insulating phases that are challenging or impossible to deposit using conventional CS systems.

### 5. Conclusion, Limitations and Future Work

This study presents the first characterization of surface morphology for cold spray depositions using vented nozzle architecture, demonstrating highly consistent Gaussian profile distributions ( $R^2 = 0.9340\text{--}0.9905$ ) regardless of process parameters and suggesting preservation of fundamental deposition mechanisms despite altered gas flow dynamics. Successful niobium deposition at  $200^\circ\text{C}$ , more than  $250^\circ\text{C}$  below conventional requirements, validates the low-temperature processing capabilities of this design, while systematic evaluation revealed complex relationships between spray passes and deposit amplitude alongside consistent jet expansion effects on profile width.

Future work will pursue several critical directions to advance understanding and application of vented nozzle technol-

Table 4: Cold Spray Gaussian Fit

SOD (mm)	Passes	A	Std. of A	$\sigma$	Std. of $\sigma$	$R^2$	Std. of $R^2$
5.25	2	46.85	1.51	3.831	0.109	0.9748	0.0018
5.25	6	39.49	1.47	2.966	0.107	0.9727	0.0042
5.25	10	48.15	2.20	3.283	0.139	0.9830	0.0041
8.75	2	63.33	0.85	4.087	0.063	0.9864	0.0023
8.75	6	38.23	1.91	3.449	0.161	0.9672	0.0110
8.75	10	52.93	3.43	3.384	0.172	0.9845	0.0023
17.5	2	59.74	2.52	4.473	0.159	0.9842	0.0050
17.5	6	28.01	2.81	3.375	0.142	0.9340	0.0120
17.5	10	88.89	5.22	4.958	0.254	0.9905	0.0024

ogy. Additional experimental rounds are necessary to establish statistical significance beyond the current single factorial design iteration. Focused Ion Beam cross-sectioning analysis is currently being explored to comprehensively characterize microstructural features, quantify porosity levels, examine particle interfaces and deformation behavior, and validate apparent density observations from optical methods. Expansion of the parameter space, including systematic exploration of lower operating pressures, expanded temperature ranges, a direct comparison between De Laval and vented nozzle architectures, and investigation of alternative propellant gases, will allow for determination of an optimal parameter set for vented nozzle CS deposition of Niobium, and establish a general methodology applicable to a broader range of materials. Lower operating pressure regimes warrant investigation following an observation during experimental operations, where depositions at 218 psi (15 bar) exhibited characteristic Gaussian profiling. While additional testing is needed this suggests the potential for low-temperature, low-pressure processing that would substantially expand material compatibility. Finally, development of predictive models, ranging from baseline regression approaches, establishing fundamental relationships, to advanced machine learning algorithms, capturing complex parameter interactions, will accelerate process development, enable configuration optimization, and support implementation of vented nozzle technology in industrial CS additive manufacturing applications.

### Acknowledgments and Declaration

The authors thank the Army Research Lab for supporting this work through grant number W911NF-24-2-0007. During the preparation of this work, the author(s) used Claude.ai 4.5 Sonnet to assist in generating Python scripts for the distribution fitting presented in Tables 2 and 3 and grammar checking. However, all the original Python codes were written by the authors, and these tools were never used as a substitute for human critical thinking, expertise, and evaluation. After using this tool, the authors reviewed and edited the content as needed and take full responsibility for the content of the published article.

### References

- [1] Akedo, J., 2008. Room temperature impact consolidation (rtic) of fine ceramic powder by aerosol deposition method and applications to microdevices. *Journal of Thermal Spray Technology* 17, 181–198.
- [2] Assadi, H., Kreye, H., Gärtner, F., Klassen, T., 2016. Cold spraying—a materials perspective. *Acta Materialia* 116, 382–407.
- [3] Bierschenk, S.G., Kovar, D., 2024a. Micro-cold spray deposition of ysz films from ultrafine powders using a pressure relief channel nozzle. *Journal of Thermal Spray Technology* 33, 2022–2033.
- [4] Bierschenk, S.G., Kovar, D., 2024b. A nozzle design for mitigating particle slowing in the bow shock region during micro-cold spray of 8 ysz films. *Journal of Aerosol Science* 179, 106360.
- [5] Cai, Z., Deng, S., Liao, H., Zeng, C., Montavon, G., 2014. The effect of spray distance and scanning step on the coating thickness uniformity in cold spray process. *Journal of thermal spray technology* 23, 354–362.
- [6] Champagne, V.K., Helfritch, D.J., Dinavahi, S.P.G., Leyman, P.F., 2011. Theoretical and experimental particle velocity in cold spray. *Journal of thermal spray technology* 20, 425–431.
- [7] Chen, C., Xie, Y., Verdy, C., Liao, H., Deng, S., 2017. Modelling of coating thickness distribution and its application in offline programming software. *Surface and Coatings Technology* 318, 315–325.
- [8] Chen, S., Bierschenk, S., Kovar, D., Sha, Z., 2025. Constrained bayesian optimization for robust design of complex systems under varying operating conditions, in: *ASME International Design Engineering Technical Conferences and Computers and Information in Engineering Conference*, p. V03BT03A024.
- [9] Earl A. Gulbransen, K.F.A., 1958. Oxidation of niobium between 375°C and 700°C. *The Electrochemical Society* 105, 4–9.
- [10] Falco, R., Bagherifard, S., 2025. Cold spray additive manufacturing: A review of shape control challenges and solutions. *Journal of Thermal Spray Technology* , 1–19.
- [11] Gärtner, F., Stoltenhoff, T., Schmidt, T., Kreye, H., 2006. The cold spray process and its potential for industrial applications. *Journal of Thermal Spray Technology* 15, 223–232.
- [12] Hanft, D., Exner, J., Schubert, M., Stöcker, T., Fuierer, P., Moos, R., 2015. An overview of the aerosol deposition method: Process fundamentals and new trends in materials applications. *J. Ceram. Sci. Technol* 6, 147–182.
- [13] Ikeuchi, D., Vargas-Uscategui, A., Wu, X., King, P.C., 2019. Neural network modelling of track profile in cold spray additive manufacturing. *Materials* 12, 2827.
- [14] Ikeuchi, D., Vargas-Uscategui, A., Wu, X., King, P.C., 2021. Data-efficient neural network for track profile modelling in cold spray additive manufacturing. *Applied Sciences* 11, 1654.
- [15] Ikeuchi, D., Vargas-Uscategui, A., Wu, X., King, P.C., 2024. Data-driven overlapping-track profile modeling in cold spray additive manufacturing. *Journal of Thermal Spray Technology* 33, 530–539.
- [16] Klinkov, S., Kosarev, V., Ryashin, N., Shikalov, V., 2018. Influence of particle impact angle on formation of profile of single coating track during cold spraying, in: *AIP Conference Proceedings*, p. 020007.
- [17] Klinkov, S., Kosarev, V., Shikalov, V., 2019. Control of cold spray process by changing of nozzle setting angle, in: *AIP Conference Proceedings*, p. 020022.
- [18] Leigh, S., Berndt, C., 1997. Evaluation of off-angle thermal spray. *Surface and Coatings technology* 89, 213–224.
- [19] Li, C.J., Wang, H.T., Zhang, Q., Yang, G.J., Li, W.Y., Liao, H., 2010. Influence of spray materials and their surface oxidation on the critical velocity in cold spraying. *Journal of Thermal Spray Technology* 19, 95–101.
- [20] Nault, I.M., Ferguson, G.D., Nardi, A.T., 2021. Multi-axis tool path optimization and deposition modeling for cold spray additive manufacturing. *Additive Manufacturing* 38, 101779.
- [21] Papyrin, A., Kosarev, V., Klinkov, S., Alkhimov, A., Fomin, V.M., 2006. *Cold spray technology*. Elsevier.
- [22] S. Kumar, A.S. Dhavale, N.M.C.S.A., 2022. Superconducting niobium coating deposited using cold spray. *Materials Letters* 312.
- [23] S. Kumar, A. Jyothirmayi, N.W.S.J., 2016. Influence of annealing on mechanical and electrochemical properties of cold sprayed niobium coatings. *Surface and Coatings Technology* 296, 124–135.
- [24] Trifa, F.I., Montavon, G., Coddet, C., 2005. On the relationships between the geometric processing parameters of aps and the al<sub>2</sub>o<sub>3</sub>-tio<sub>2</sub> deposit shapes. *Surface and Coatings Technology* 195, 54–69.
- [25] Vanerio, D., Kondas, J., Guagliano, M., Bagherifard, S., 2021. 3d modelling of the deposit profile in cold spray additive manufacturing. *Journal of Manufacturing Processes* 67, 521–534.
- [26] Villafuerte, J., 2015. *Modern cold spray*. Windsor, Ontario, Canada: Springer International Publishing .
- [27] Wu, H., Li, W., Lewke, M., Deng, S., List, A., Gaertner, F., Klassen, T., 2024. 3d volume construction methodology for cold spray additive manufacturing. *Additive Manufacturing* 92, 104407.
- [28] Wu, H., Xie, X., Liu, M., Chen, C., Liao, H., Zhang, Y., Deng, S., 2020. A new approach to simulate coating thickness in cold spray. *Surface and Coatings Technology* 382, 125151.
- [29] Yin, S., Cavaliere, P., Aldwell, B., Jenkins, R., Liao, H., Li, W., Lupoi, R., 2018. Cold spray additive manufacturing and repair: Fundamentals and applications. *Additive manufacturing* 21, 628–650.